

UDC 621.371

doi:10.15217/issn1684-8853.2018.1.74

IMPACT OF BUILT-UP TERRAIN ON OPERATIONAL PARAMETERS OF SIGNALS IN LAND-SATELLITE COMMUNICATION LINKS

N. S. Blaunstein^a, Dr. Sc., Phys.-Math., Professor, nathan.blaunstein@hotmail.com

M. B. Sergeev^b, Dr. Sc., Tech., Professor, mbse@mail.ru

V. A. Nenashev^b, PhD, Tech., Assistant Professor, nenashev.va@gmail.com

^aBen-Gurion University of the Negev, P.O.B. 653, 1, Ben-Gurion St., Beer-Sheva, 74105, Israel

^bSaint-Petersburg State University of Aerospace Instrumentation, 67, B. Morskaya St., 190000, Saint-Petersburg, Russian Federation

Purpose: Examining the propagation of radio signals in urban environments for different elevations of a moving satellite antenna and stationary or mobile subscribers' antennas located below or above the rooftops, based on a stochastic multi-parametric approach and concentrating on temporal and spatial properties of signal power variations in order to predict the channel pass loss and fading effects. **Results:** In the framework of the stochastic approach proposed in this work, the total signal power, the corresponding probability density functions, and the scales of the temporal and frequency characteristics were analyzed. All the predicted characteristics were examined numerically. The impact of buildings' density and satellite antenna elevation upon the above-mentioned characteristics of the radio signal were examined through the lens of special experiments performed by various research groups worldwide. **Practical relevance:** As the computed and experimentally observed data give a good agreement between the proposed stochastic approach and the approaches proposed by other researchers, it can be used to predict link budget for various built-up terrain environments and for various elevations of moving satellite antennas.

Keywords — Land-Satellite Link, Stochastic Multi-Parametric Model, Buildings' Density and Overlay Profile, Multiplicative Fading Probability, Pass Loss, Link Budget.

Citation: Blaunstein N. S., Sergeev M. B., Nenashev V. A. Impact of Built-up Terrain on Operational Parameters of Signals in Land-Satellite Communication Links. *Informatsionno-upravliayushchie sistemy* [Information and Control Systems], 2018, no. 1, pp. 74–84. doi:10.15217/issn1684-8853.2018.1.74

Introduction

From the middle of the 20th century worldwide researchers tried to find the adequate models that could predict operational parameters, pass loss, fading and link budget, in the land-satellite communication (LSC) links where the built-up profile, density of buildings and other obstructions, as well as the terrain structure and contours affect signals passing from the moving satellite and ground-located subscriber. Where proposed several approaches that we briefly will present below to understand the matter of the problem under studying. In our description of the matter we follow results discussed in the references [1–27].

Statistical Models

These models correspond to cases for which multipath and line-of-sight are present simultaneously [6–13, 16, 19]. In this section we will describe only two models; Loo's [15, 17] and Lutz [16], which have been used in [10, 11, 22, 23] for designing the unified algorithm for predicting fading phenomena in the land-satellite links. Therefore, we will describe briefly these models and compare their results with those obtained in [10, 11, 22, 23] and with those obtained on the basis of the multi-parametric stochas-

tic approach proposed for the land-satellite links in [20] for the special series of experiments described in [11, 25–27].

We also refer the reader to some other statistical models by Corazza — Vatalaro [19], Xia — Fang [20], Abdi [21], and the three-state model [27], which are lesser used by designers of such land-satellite links.

Loo's Model. This model is a statistical model [15, 17] for a land mobile-satellite link with applications to rural environments. The model assumes that the amplitude of the line-of-sight (LOS) component under foliage attenuation is distributed according to the lognormal probability density function (PDF) and the received multipath component is described by a Rayleigh PDF. The model is statistically described in terms of its PDF or cumulative distribution function (CDF), which were obtained under the hypothesis that foliage not only attenuates but also scatters radio waves. In such assumptions, the total complex fading signal is the sum of a lognormally distributed random signal and a Rayleigh signal [15, 17]:

$$r \exp(j\theta) = z \cdot \exp(j\varphi_0) + w \cdot \exp(j\varphi), \quad z > 0, w > 0, \quad (1)$$

where the phase φ_0 and φ are uniformly distributed between 0 and 2π ; z is lognormal distributed

amplitude, and w is a Rayleigh distributed amplitude. If z is temporally kept constant, it can be assumed that the PDF $p(z)$ is lognormal. The signal random envelope r is lognormal distributed for large values and Rayleigh distributed for small values [15, 17]:

$$p(r) \approx \begin{cases} \frac{1}{r\sqrt{2\pi d_0}} \exp\left[-\frac{(\ln r - \mu)^2}{2d_0}\right] & \text{for } r \gg \sqrt{d_0} \\ \frac{r}{b_0} \exp\left[-\frac{r^2}{2b_0}\right] & \text{for } r \ll \sqrt{b_0} \end{cases} \quad (2)$$

In this equation $\sqrt{d_0}$ and μ are the standard deviation and mean for the lognormal distribution, and b_0 is the variance for the Rayleigh distribution, respectively. The parameter b_0 represents also the average scattered power caused by multipath effects.

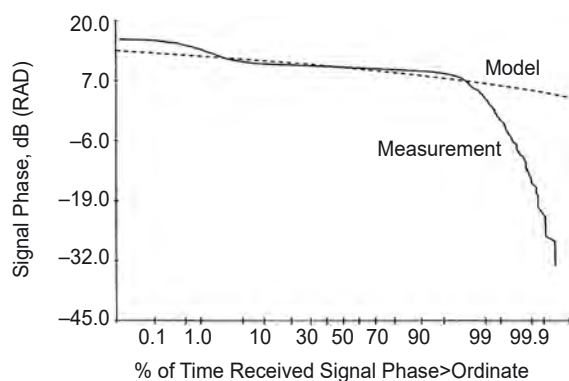
Many calculations with different values for b_0 , d_0 and μ where carried out by Loo with the objective of fitting the results of his model to those derived from measurements made on simulated satellite paths. The measurements site was a rural area with about 35 % tree coverage. The model parameters were obtained by trial and error to fit measured values.

Computational results for the signal envelope, based on Loo's model, we compare to measurements obtained in [15, 17].

As was mentioned in [8], the signal envelope PDF of the model facilitates the calculation of fade margins in the design of communications systems. As for the signal envelope phase distribution, Fig. 1 shows a comparison of the complementary cumulative distribution function (CCDF) for the received signal phase calculated using the well-known equation [8]:

$$CCDF(r) \equiv p(r > R) = 1 - CCD(r) = 1 - \int_0^R p(r) dr, \quad (3)$$

where R is either maximum accepted path loss or noise floor figure of the system.



■ Fig. 1. Loo's phase model and measurement for heavy shadowing at $f = 18.925$ GHz

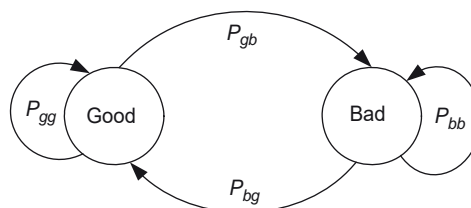
We must note that for the case of infrequent light shadowing, the model shows the best fit around the median region and some deviation near the tails of the distribution. As for the heavy shadowing situation is changed (see Fig. 1), the results indicate that the model shows a correlation between the rate of change of the envelope due to multipath and foliage attenuation for heavy shadowing too excluding only the higher probability of the event. The disadvantage of this model is that the measurements were made up to 30°. Model parameters for higher elevation angles are not available.

Lutz Statistical Model. In this model, which can be considered as a generalization of the Loo's model, the simple statistics of LOS and NLOS (non-line-of-sight) are modeled by two distinct states, *good* and *bad*, called the *Markov's chain*, as shown in Fig. 2. This is appropriate for describing the propagation situation in urban and sub-urban areas where there is a large difference between the shadowed and non-shadowed statistics. The parameters associated with each state and the transition probabilities for evolution between states are empirically derived. The LOS condition is represented by a good state, and the NLOS condition by a bad state. In the good state, the signal is assumed to be Ricean K -factor distributed [8], which depends on the satellite elevation angle and the carrier frequency, so that the PDF of the signal amplitude is given by $P_{good} = P_{Rice}$. In the bad state, the fading statistics of the signal amplitude are assumed to be Rayleigh, with a mean power $S_0 = \sigma^2$, which varies with time.

So the PDF of amplitude is specified as the conditional distribution $p_{Rayleigh}(S|S_0)$, where S_0 varies slowly with a lognormal distribution $p_{LN}(S_0)$, representing the varying effects of shadowing with the NLOS component. For detailed formulas, we refer the reader to the original [8].

Transitions between states are described by a first-order Markov chain. This is a state transition system, in which the transition from one state to another depends only on the current state rather than on any more distant history of the system. The transition probabilities, which summarize all models based on the Markov chain approach, are (see Fig. 2 [8]):

- from good state to good state P_{gg} ;
- from good state to bad state P_{gb} ;



■ Fig. 2. Markov's model of channel states

from bad state to bad state P_{bb} ;
 from bad state to good state P_{bg} .

For a digital communication system, each state transition is taken to represent the transition of one symbol. The transition probabilities can then be found in terms of the mean number of symbol duration spent in each state [8]:

$$P_{gb} = \frac{1}{D_g} \text{ where } D_g \text{ is the mean number of symbol duration in the good state;}$$

$$P_{bg} = \frac{1}{D_b} \text{ where } D_b \text{ is the mean number of symbol duration in the bad state.}$$

The sum of the probabilities leading from any state must equal to the sum of

$$P_{gg} = 1 - P_{gb} \text{ and } P_{bb} = 1 - P_{bg}. \quad (4)$$

The time share of shadowing (the proportion of a symbol in the bad state) is

$$A = \frac{D_b}{D_g + D_b}. \quad (5)$$

Below we will use this formula to find the parameter A , denoted as *the time share of shadowing*, during comparison with physical-statistical and the stochastic multiparametric approaches, where this parameter is derived in other manner. In this comparison we will use the Lutz model as a classical statistical approach.

Physical-Statistical Models

In pure statistical models, the input data and computational effort are quite simple, as the model parameters are fitted to measured data. Such models only apply to hypothetical environments and lack the physical background of the realistic problem. On the other hand, pure deterministic physical models provide high accuracy, but they require actual analytical path profiles and time-consuming computations.

A combination of both approaches has been developed by the authors. The general method relates any channel simulation to the statistical distribution of physical parameters, such as building height, width and spacing, street width or elevation and azimuth angles of the satellite link. This approach is henceforth referred to as the *“Physical-Statistical”* approach [10, 11, 22, 23]. The main concept of such an approach is the following. According to the *physical* approach, input knowledge consists of electromagnetic theory and a full physical understanding of the propagation processes. However, this knowledge is then used to analyze a *statistical*

input data set, yielding a *distribution* of the output predictions. The output predictions are not linked to specific locations. Physical-statistical approach therefore require only simple input data such as distribution parameters (e. g., mean building height and building height variance).

This model describes the geometry of mobile satellite propagation in built-up areas and proposes statistical distributions of building heights, which are used in subsequent analysis. We will consider only two these models:

1) a shadowing model based on the two-state channel Lutz model;

2) a multi-parametric stochastic model.

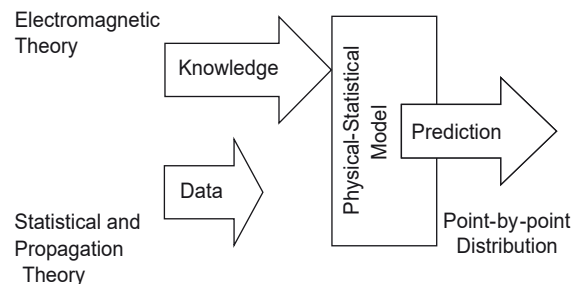
The Model of Shadowing. The geometry of the situation, which was analyzed in [10, 11, 22, 23] by Saunders and Evans with their colleagues, is illustrated in Fig. 3.

It describes a situation where a mobile is situated along a straight street with the direct ray from the satellite impinging on the mobile from an arbitrary direction. The street has buildings, line-up on both sides, with randomly varying heights. In the presented model, the statistics of building height in typical built-up areas is used as input data. A suitable form was sought by comparing with geographical data for the cities of Westminster and Guildford, UK [11, 22, 23]. The PDFs that were selected to fit the data are the log-normal and Rayleigh distributions with unknown parameters the mean value, m , and standard deviation, σ_b . The PDF for the log-normal distribution is [10, 22, 23]

$$p_b(h_b) = \frac{1}{h_b \sqrt{2\pi} \sigma_b} \cdot e^{-\frac{\ln^2(h_b/m)}{2\sigma_b^2}}. \quad (6)$$

The PDF for the Rayleigh distribution is fully described in [8]. We will repeat it using notations made in references [10, 22, 23]:

$$p_b(h_b) = \frac{h_b}{\sigma_b^2} \cdot e^{-\frac{h_b^2}{2\sigma_b^2}}. \quad (7)$$



■ Fig. 3. Algorithm of physical-statistical model

■ **Table 1.** Best-fit parameters for the theoretical PDFs

City	Lognormal PDF		Rayleigh PDF
	Mean m	Standard Deviation	Standard Deviation
Westminster	20.6	0.44	17.6
Guildford	7.1	0.27	6.4

To find the appropriate parameters for these functions in order to fit the data measurements as accurately as possible, the PDF was found by minimizing the maximum difference between the two cumulative distribution functions. The parameters for each PDF are quoted in Table 1 from [10, 22, 23], where all parameters are in meters.

The direct ray is judged to be shadowed when the building height h_b exceeds some threshold height h_T relative to the direct ray height h_s (Fig. 4). The shadowing probability, P_s , can then be expressed in terms of the PDF of the building height, $p_b(h_b)$ as [10, 22, 23]

$$P_s = \Pr(h_b > h_T) = \int_{h_T}^{\infty} p_b(h_b) dh_b. \quad (8)$$

The definition of h_T is obtained by considering shadowing to occur exactly when the direct ray is geometrically blocked by the building face. Using a simple geometry, the following expression is extracted for h_T [10, 22]:

$$h_T = h_r = \begin{cases} h_m + \frac{d_m \tan \varphi}{\sin \theta} & \text{for } 0 < \theta < \pi \\ h_m + \frac{(w - d_m) \tan \varphi}{\sin \theta} & \text{for } -\pi < \theta < 0 \end{cases}. \quad (9)$$

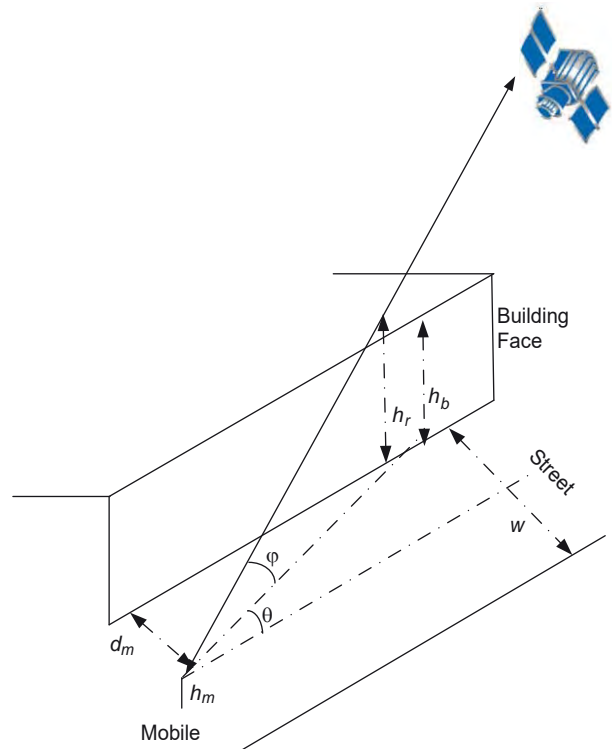
All notations and geometrical parameters in (9) are explained in Fig. 4.

The shadowing model estimates the probability of shadowing for Lutz two-state model [24]. The same Markov chain, shown in Fig. 2, is used, but parameters A , P_{bad} and P_{good} are obtained from actual random distribution of the obstructions above the terrain. Thus,

$$A = \int_{z_1}^{z_2} P_b(h) dh, \quad (10)$$

where h are different heights of obstacles, z_1 and z_2 are the minimum and maximum height of the built-up layer;

$$P_b = \begin{cases} \text{lognormal} + \text{Ricean} \\ \text{lognormal} + \text{Rayleigh} \end{cases}, \quad (11)$$


 ■ **Fig. 4.** Geometry for mobile-satellite communication in built-up areas

where the lognormal PDF is for pure NLOS shadowing. The Ricean PDF describes both the LOS and the multipath component, and the Rayleigh PDF describes the multipath component of the total signal, when the LOS component is absent [8].

Now, using theoretical results obtained by Lutz's pure statistical model and results the Saunders and Evans model, we can combine them into one unified model. This unified model will be compared with the stochastic multiparametric model described in the next section based on the theoretical framework analyzed in [8]. Thus, taking into account the Markov's chain (see Fig. 2), we consider the *bad state* by using the Rayleigh PDF and the *good state* by using the Ricean PDF, as well as shadowing by using the lognormal PDF. By combining all these PDFs in a Markov's chain, we finally can obtain the total PDF that describes the effects of different kinds of fading occurring within the LSC link, caused by terrain obstructions; natural and man-made. As a result we get

$$p(S) = (1 - A) \cdot P_{good} + A \cdot P_{bad} = (1 - A) \cdot P_{Rice}(S) + A \int_0^{\infty} p_{Rayleigh}(S | S_0) \cdot p_{lognorm}(S_0) dS_0. \quad (12)$$

Then, we introduce the corresponding CCDF, which describes the signal stability, being the received signal with amplitude r that prevails upon the maximum accepted path loss, R , in the mul-

tipath channel, caused by fading phenomena. This can be presented in the following form:

$$CCDF = \Pr(r > R) = \int_0^R p(S) dS. \quad (13)$$

All above formulas allow us to present the unified algorithm for fading phenomena estimation in LSC links, both stationary and mobile.

Multi-Parametric Stochastic Approach

As an example of a physical-statistical model, we present the same stochastic approach which was used successfully for land communication channels, rural, sub-urban and urban, and was described in [1–8]. The reason for that is based on the fact that the previous physical-statistical model, as was shown in [10, 11, 22, 23], predicts more strictly the fading effects in different LSC links compared to the pure statistical models [15–21].

At the same time, as was mentioned in [8], the physical-statistical model, which is based on a deterministic distribution of the local built-up geometry introduced in [22, 23], cannot strictly predict any situation when a satellite, moving around the world, has different elevation angles θ_i with respect to a subscriber located at the ground surface, as shown in Fig. 5. As the result, the radio path between the desired subscriber and the satellite crosses different overlay profiles of the buildings because of continuously changing elevation angle of the satellite during its rotation around the Earth with respect to the ground-based subscriber anten-

na. To predict continuously the outage probability of shadowing in real time, a huge amount of data is needed regarding each building, geometry of each radio path between desired user and the satellite during its rotation around the Earth, and finally high-speed powerful computer.

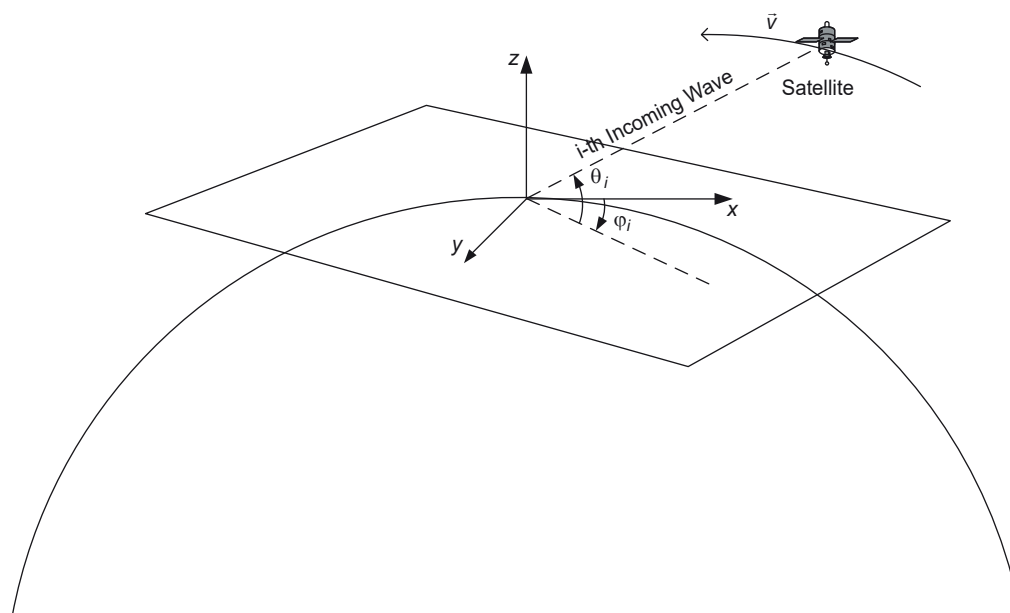
Most of these difficulties can be handled by using the multi-parametric stochastic model [1–8]. Following [8], we take into account both, the buildings distribution at the ground surface and their height profile changing in the vertical plane that is, accounting for the 3D stochastic model of multiple scattering, reflection and diffraction rearranging the corresponding formulas in the case of the LSC link.

Buildings' Overlay Profile. The LSC link is very sensitive to the overlay profile of the buildings, because during its movement around the Earth, depending on the elevation angle φ , the buildings' profile will be continuously changed leading to different effects of shadowing in the current communication link (Fig. 6).

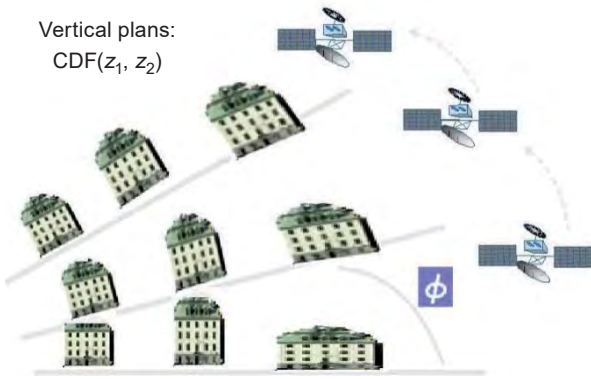
Taking into account the fact that real profiles of urban environment are randomly distributed, the probability function $P_h(z)$, which describes the overlay profile of the buildings, can be presented in the following form [6, 20, 39]:

$$P_b(z) = H(h_1 - z) + H(z - h_1) \cdot H(h_2 - z) \times \left[\frac{(h_2 - z)}{(h_2 - h_1)} \right]^n, \quad n > 0, \quad 0 < z < h_2, \quad (14)$$

where the function $H(x)$ is the Heaviside step function, which is equal 1, if $x > 0$, and is equal 0, if $x < 0$.



■ Fig. 5. General geometry of the land-satellite link



■ Fig. 6. Change of the profile function $F(z_1, z_2)$ in the vertical plane during the movements of a satellite

The graph of this function versus height z of a built-up overlay is presented in Fig. 7. For $n \gg 1$ $P_b(z)$ describes the case where buildings higher than h_1 (minimum level) very rarely exist. The case, where all buildings have heights close to h_2 (maximum level of the built-up layer), is given by $n \ll 1$. For n close to zero, or n approaching infinity, most buildings have approximately the same level that equals h_2 or h_1 , respectively. For $n = 1$, we have the case of building height uniformly distributed in the range of h_1 to h_2 .

The average buildings height \bar{h} , can be found as [8]

$$\bar{h} = h_2 - n \frac{(h_2 - h_1)}{n + 1}. \quad (15)$$

Then, analyzing the built-up layer profile $F(z_1, z_2)$, “illuminating” by the terminal antennas of the heights z_1 and z_2 , we get :

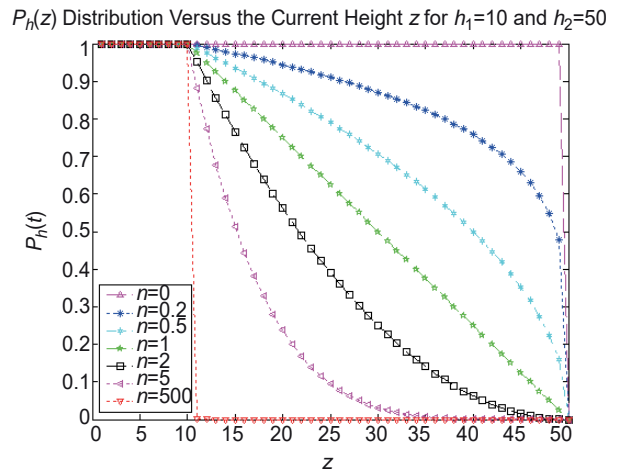
— for the case when the antenna height is above the rooftop level, that is, $z_2 > h_2 > h_1$:

$$F(z_1, z_2) = H(h_1 - z_1) \left[(h_1 - z_1) + \frac{(h_2 - h_1)}{(n + 1)} \right] + H(z_1 - h_1) H(h_2 - z_1) \frac{(h_2 - z_1)^{n+1}}{(n + 1)(h_2 - h_1)^n}; \quad (16a)$$

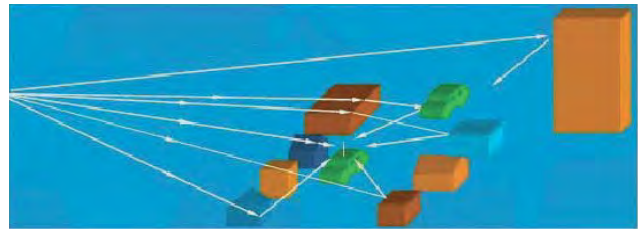
— for the case when the antenna height is below the rooftop level, that is, $z_2 < h_2$:

$$F(z_1, z_2) = H(h_1 - z_1) \times \left[(h_1 - z_1) + \frac{(h_2 - h_1)^{n+1} - (h_2 - z_2)^{n+1}}{(n + 1)(h_2 - h_1)^n} \right] + H(z_1 - h_1) H(h_2 - z_1) \frac{(h_2 - h_1)^{n+1} - (h_2 - z_2)^{n+1}}{(n + 1)(h_2 - h_1)^n}. \quad (16b)$$

Then, the cumulative distribution probability function (CDF) of the event that any subscriber



■ Fig. 7. Buildings’ overlay profile PDF



■ Fig. 8. Horizontal map of multipath phenomenon occurring in the urban scene

located in the built-up layer is affected by obstructions due to shadowing effect can be presented as [1–8]

$$CDF(z_1, z_2, n) = \frac{1}{z_2 - z_1} \int_{z_1}^{z_2} P_h(z) dz \equiv \frac{1}{z_2 - z_1} F(z_1, z_2). \quad (17)$$

The built-up profile function presented by (16) allows us to account for continuous changes of the overlay building profile during the movement of the satellite around the Earth and the corresponding changes of its elevation angle with respect to the position of any subscriber located in areas of service. This CDF will be used in the next section to find the total outage probability of fading phenomena occurring in LSC links.

Multi-ray Pattern Distribution on the Ground Surface. As is shown in [1–7] and mentioned also in [8], at the horizontal plane the array of buildings are randomly distributed according to Poisson’s law. During movement around the Earth, the satellite antenna “illuminates” different land areas with various distributions of obstructions on the ground surface, that is, in the horizontal plane, as shown in Fig. 8.

The proposed multi-parametric model [1–8] allows us to consider the strength of the total field at the receiver as the additive summation of n -time independently scattered waves with independent strengths. The real situation with multipath phenomena occurring in the urban environment is shown in Fig. 8. As was mentioned in [8], in micro-cell land communication links ($d < 1\text{--}3$ km; d is the range from the base station antenna), the singly scattered waves are dominant, whereas the twice- and three-time scattered waves begin to prevail in macro-cell scenarios for $d > 5\text{--}10$ km. Therefore, as was shown in [8], for land-satellite mega-cell links we must additionally consider the three-time reflected and scattered waves. As was shown in [8], the strengths r_i of these waves are distributed according to the Gaussian law with the zero-mean value and dispersion σ_1^2 (for singly scattered waves), σ_2^2 (for twice scattered waves) and σ_3^2 (for three-time scattered waves), which depend strongly on the characteristic features of the terrain. The average number of scattered waves involves also a dependence on the distance from the base station antenna d . Following [8], we can obtain a new multi-ray distribution for the LSC link. Thus:

— for the average number of single scattered waves

$$\bar{N}_1 = \frac{\pi v d^2}{4} K_2(\gamma_0 d); \quad (18a)$$

— for the average number of two-time scattered waves

$$\bar{N}_2 = 9(\pi v d^2)^2 \left[\frac{K_4(\gamma_0 d)}{8!} + \sqrt{\frac{2}{\pi \gamma_0 d}} \frac{K_{7/2}(\gamma_0 d)}{7!} \right]; \quad (18b)$$

— for the average number of three-time scattered waves

$$\bar{N}_3 = 8(\pi v d^2)^3 \times \left[\frac{1}{\gamma_0 d} \frac{K_5(\gamma_0 d)}{10!} + \sqrt{\frac{2}{\pi \gamma_0 d}} \frac{K_{11/2}(\gamma_0 d)}{11!} \right], \quad (18c)$$

where $K_n(\gamma_0 d)$ is the MacDonal'd's function of n -order, γ_0 [km⁻¹] is the density of buildings contours [8].

The probability of receiving once to three-time (i. e., for $n = 1, 2, 3$) scattered waves at the mobile station antenna can be computed according to the following formula [8]:

$$P_n = 1 - \exp[-\bar{N}_n], \quad n = 1, 2, 3. \quad (19)$$

In computations of equation (19) we take into account the effects of independent single (the first term), double (the second term) and triple (the third

term) scattering of rays with the random amplitude r , as well as their mutual influences on each other (the fourth term), that is,

$$\begin{aligned} CDF(r) = & \frac{P_1(1-P_2)(1-P_3)}{P_0} \frac{r}{\sigma_1^2} e^{-\frac{r^2}{2\sigma_1^2}} + \\ & + \frac{P_2(1-P_1)(1-P_3)}{P_0} \frac{r}{\sigma_2^2} e^{-\frac{r^2}{2\sigma_2^2}} + \\ & + \frac{P_3(1-P_1)(1-P_2)}{P_0} \frac{r}{\sigma_3^2} e^{-\frac{r^2}{2\sigma_3^2}} + \\ & + \frac{P_1 P_2 P_3}{P_0} \frac{r}{\sigma_1^2 + \sigma_2^2 + \sigma_3^2} e^{-\frac{r^2}{2(\sigma_1^2 + \sigma_2^2 + \sigma_3^2)}}, \quad (20) \end{aligned}$$

where

$$P_0 = 1 - (1 - P_1)(1 - P_2)(1 - P_3) = 1 - e^{-(\bar{N}_1 + \bar{N}_2 + \bar{N}_3)} \quad (21)$$

is the probability of direct visibility (e. g., LOS component), P_1 , P_2 and P_3 are defined by equation (21) combined with (18a)–(18c), respectively.

Equation (21) is more general form of the cumulative distribution function of the multipath effects occur in the land-satellite links with respect to that describing the same multi-ray effects in the land-to-land communication scenarios (see [1–8]). This CDF will be used in the next section [together with CDF described by (19)] to estimate the total probability of fading for predicting successful communication and service by the satellite antenna of any ground-based subscriber.

Prediction of Fading and Pass Loss in LSC Links via Experimental Data

In this section, we use the unified algorithm, based on use the combination of the physical-statistical (e. g., Saunders and Evans) model and the pure statistical (Lutz) model of the mobile-satellite communication channel, using formulas (12) and (13), and compare it with the proposed stochastic multi-parametric model based on the corresponding $CCDF(r) = 1 - CDF(r)$, of signal random strength envelope (20). This CCDF describes the total probability to achieve a successful communication between any ground-based subscriber and the satellite. It can be presented as [8]

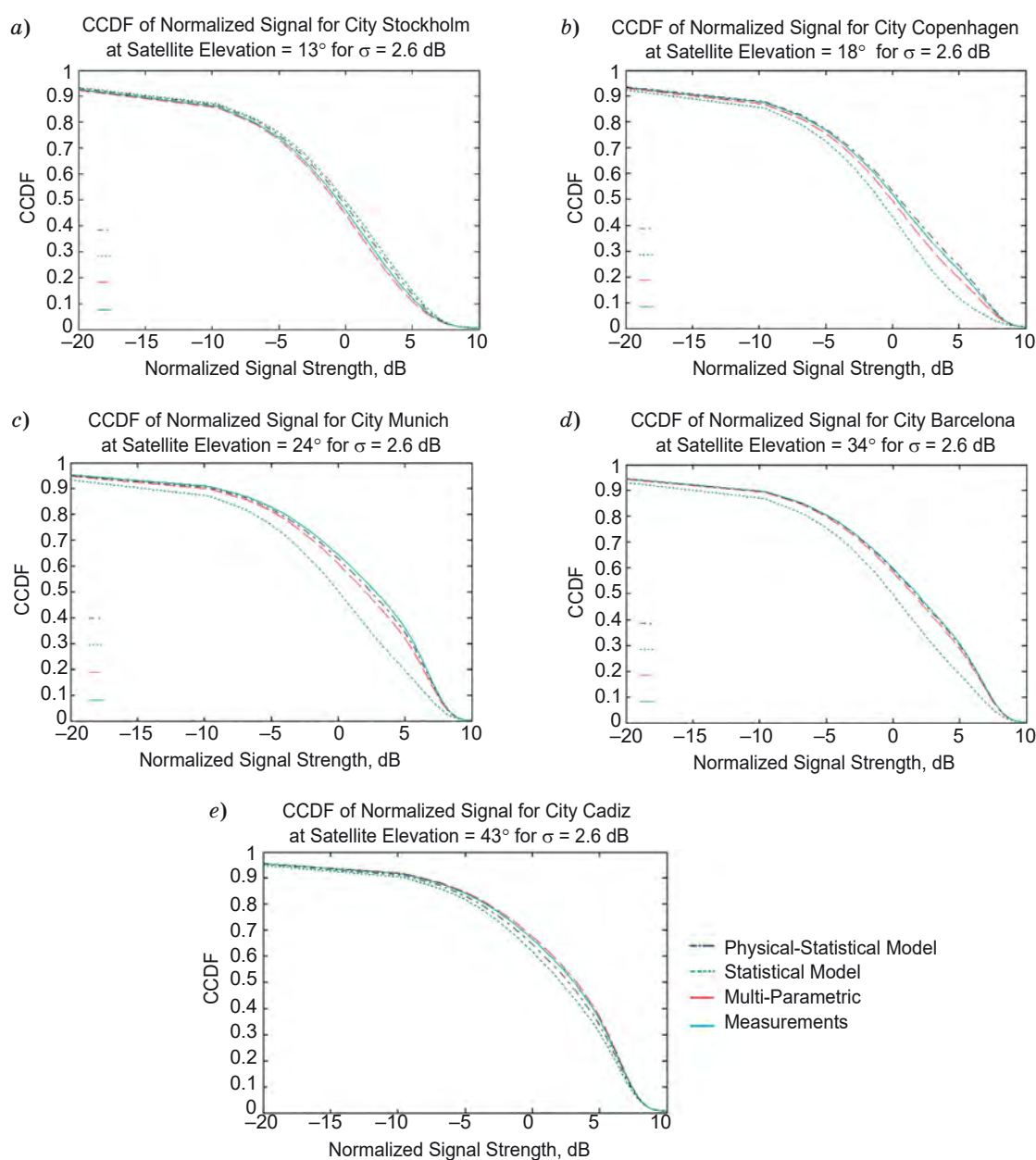
$$CCDF(r) = 1 - CDF(r) \cdot CDF(z_1, z_2, n), \quad (22)$$

where both CDFs are described by (17) and (20), respectively.

In the comparative analysis, we used measured data from references [25, 26], done in several cities in Europe. These tests were narrowband measurements at a single frequency, representing the channel within its coherence bandwidth. The test was transmitted from the ESA ground station in Villafranca, Spain and relayed by the geostationary satellite MARECS at L-band (1.54 GHz). The measurements were conducted in areas with different satellite elevations (Table 2). Using these measurements and using a Rayleigh PDF for building distribution heights and the corresponding equation (22) for CCDF, we constructed a corresponding numerical code to see if there is a good agree-

■ **Table 2.** Parameters of channel model according to [25, 26]

Satellite Elevation	A	$10\log(\epsilon)$, dB	M , dB	σ , dB
13° — Stockholm	0.24	10.2	-8.9	5.1
18° — Copenhagen	0.8	6.4	-11.8	4.0
24° — Munich	0.66	6.0	-10.8	2.8
34° — Barcelona	0.58	6.0	-10.6	2.6
43° — Cadiz	0.54	5.5	-13.6	3.8



■ **Fig. 9.** CCDF of normalized signal for three different models: *a* — for city Stockholm at satellite elevation angle 13°; *b* — for city Copenhagen at satellite elevation angle 18°; *c* — for city Munich at satellite elevation angle 24°; *d* — for city Barcelona at satellite elevation angle 34°; *e* — for city Cadiz at satellite elevation angle 43°

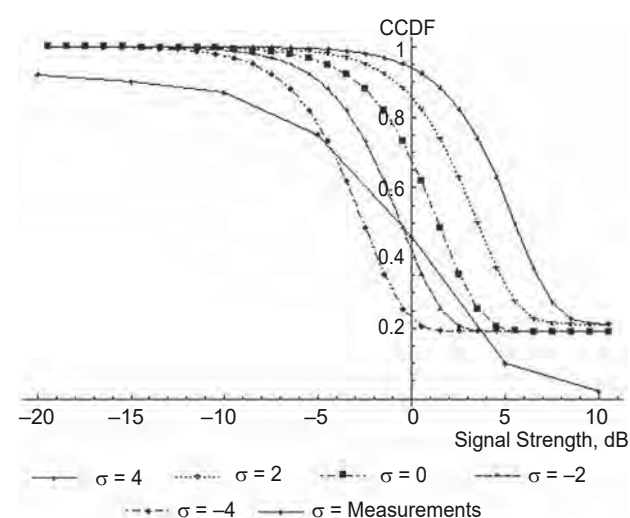
ment with the measured data. It is clear that the CCDF gives us the knowledge of stability of received signal with respect to noise caused by fading phenomena.

The same was done for the multi-parametric model by using equation (22) with the corresponding CDF (17) and (20) for each city. The results of fading estimations were compared with those obtained from the pure statistical Lutz model based on Markov's chain.

The main goal of such simulations was to define which one of the three models presented the best fit to the measured data and also the simplest one. In such a comparison we used for the Lutz statistical model simulation $P_{gg} = (0.8, 0.95, 0.85, 0.83, 0.7)$ and $P_{bb} = (0.08, 0.15, 0.25, 0.22, 0.5)$. These results are shown in Figs. 9, *a-e* for five cities presented in Table 2.

The standard deviation, σ , was taken not more than 2.6 dB, obtained from our estimations of each built-up profile. Nevertheless, in reference [16], the authors used $\sigma = 3\div 4$ dB, which is not a realistic case when NLOS regime is very small compared with the LOS component of the total field strength. It is clearly seen from the results of the comparative analysis presented in Fig. 9, *a-e* that the physical-statistical models, Saunders and Evans, and the stochastic multi-parametric, are closer to the experimental data compared to the pure statistical Lutz model. Therefore, in our further analysis, we will compare the proposed physical-statistical models with each other.

Before doing this comparative analysis, let us check the accuracy of the proposed stochastic model in the case when the standard deviation of the CCDF cannot be directly estimated via numerical evaluations. Thus, in Fig. 10, the CCDF of received signal for the city of Stockholm [25–27], at satellite



■ Fig. 10. Comparison between the experimental data obtained in satellite observations over Stockholm (continuous line) and those obtained theoretically from the stochastic approach

elevation angle 13° is presented. The computations were carried out taking the following parameters:

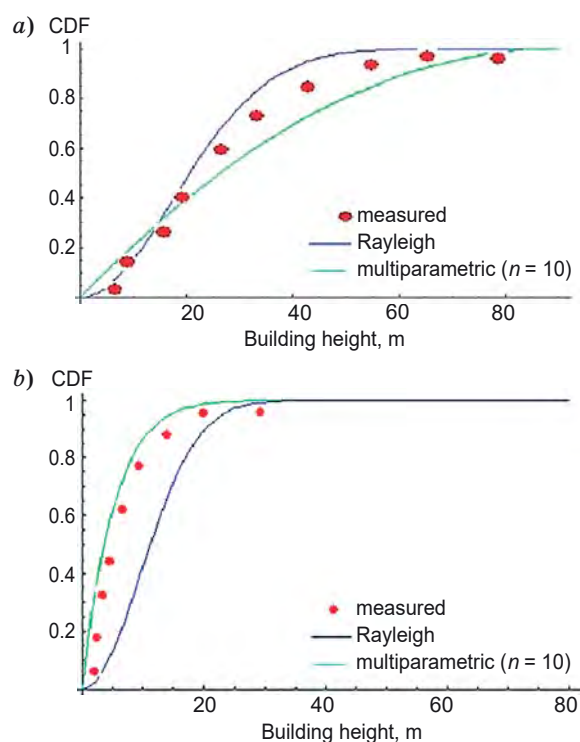
- the building contour density parameter varied from 8 to 12 km^{-1} with the mean value $\bar{\gamma}_0 = 10 \text{ km}^{-1}$;
- the built-up profile parameter n was changed from 0.65 to 1.48;
- the obtained terrain data allow us to estimate the standard deviation of CCDF within the range of $\sigma \in (-4, 4)$ dB.

The results of comparison between the experimental data (continuous curve) and those obtained numerically for the range in the estimated parameters σ shown in Fig. 9 show that the experimental data lie between the two theoretical curves computed for σ changing from -4 to -2 dB, which is close to that parameter estimated by analyzing the topographic map of Stockholm [25–27].

Another land-satellite experiment was compared with the Saunders — Evans physical-statistical model [10, 11, 22, 23], and was carried out in England for two cities, Westmister and Guildford. Here, the CDF, as a total probability of shadowing was investigated using both models. We do not go deeply into the description of these experiments that are fully described in [10, 11, 22, 23]. Here we will only mention that a comparison showed that the best fit was obtained when the CDF of the combined fast/slow fading was described by the corresponding Rayleigh law with the corresponding mean height of buildings $\bar{h} = 20.6$ m and standard deviation $\sigma_b = 17.6$ m (for Westmister) and $\bar{h} = 7.6$ m and $\sigma_b = 6.4$ m (for Guildford). The corresponding comparison analysis is presented in Fig. 11, *a* and *b* for each city, respectively.

Therefore, in this additional comparison with the Saunders — Evans, physical-statistical model and with experimental data, we accounted for these estimations as well as for the average density of buildings' contours within one square kilometer, which was estimated as $\bar{\gamma}_0 \approx 10.6 \text{ km}^{-1}$ (for Westmister) and $\bar{\gamma}_0 \approx 7.5 \text{ km}^{-1}$ (for Guildford). We also estimated the corresponding mean height of buildings for Westmister, $\bar{h} = 18.2$ m with a standard deviation of $\sigma_b = 7.5$ m and for Guildford, $\bar{h} = 5.8$ m and $\sigma_b = 4.6$ m. These estimations have suggested that the two cities have fully different built-up terrain profiles: the parameter of the overlay building profile is $n = 2$ (the amount of small buildings exceeds that of tall buildings) for Westmister, and $n = 10$ (most buildings are small) for Guildford.

We should note that these parameters were taken in a form of average values, but not exactly, as was done by Saunders and Evans with their co-authors in [10, 11, 22, 23] using the local parameters for each position of the moving satellite. Despite this fact, our estimations are within the ranges of estimations obtained by Saunders and Evans, and we can, finally, compare our computations of $CDF = 1 - CCDF$ according to (17), (20) and (22) with those obtained by them using the Rayleigh CDF, as a best fit of measu-



■ **Fig. 11.** Comparison between experimental data (dots) obtained in Westminster (a) and Guildford (b), physical statistical model (blue line) and data obtained from the stochastic approach (green line)

References

1. Blaunstein N., and Christodoulou Ch. G. *Radio Propagation and Adaptive Antennas for Wireless Communication Links — Terrestrial, Atmospheric and Ionospheric*. Hoboken, New Jersey, Wiley Interscience, 2007. 614 p.
2. Blaunstein N. Prediction of Cellular Characteristics for Various Urban Environments. *IEEE Anten. Propag. Magazine*, 1999, vol. 41, no. 6, pp. 135–145.
3. Blaunstein N. D., Katz D., Censor, et al. Prediction of Loss Characteristics in Built-up Areas with Various Buildings' Overlay Profiles. *IEEE Anten. Propag. Magazine*, 2001, vol. 43, no. 6, pp. 181–191.
4. Blaunstein N. Distribution of Angle-of-Arrival and Delay from Array of Buildings Placed on Rough Terrain for Various Elevations of Base Station Antenna. *J. Commun. and Networks*, 2000, vol. 2, no. 4, pp. 305–316.
5. Blaunstein N., Toulch M., Laurila J., Bonek E., et al. Signal Power Distribution in the Azimuth, Elevation and Time Delay Domains in Urban Environments for Various Elevations of Base Station Antenna. *IEEE Trans. Anten. and Propagat.*, 2006, vol. 54, no. 10, pp. 2902–2916.
6. Blaunstein N., Yarkoni N., and Katz D. Spatial and Temporal Distribution of the VHF/UHF Radio Waves in Built-up Land Communication Links. *IEEE Trans. Anten. and Propagat.*, 2006, vol. 54, no. 8, pp. 2345–2355.
7. Blaunstein N., and Ben-Shimol Y. Spectral Properties of Signal Fading and Doppler Spectra Distribution in Urban Mobile Communication Link. *J. Wireless Commun. and Mobile Comput.*, 2006, vol. 6, no. 1, pp. 113–126.
8. Blaunstein N., and Christodoulou Ch. G. *Radio Propagation and Adaptive Antennas for Wireless Communication Networks — Terrestrial, Atmospheric and Ionospheric*. Boca Rocha, Florida, Wiley, 2014. 704 p.
9. Farserotu J., Prasad R. *IP/ATM Mobile Satellite Networks*. Artech House, 2002. 289 p.
10. Saunders S. R. *Antennas and Propagation for Wireless Communication Systems*. John Wiley & Sons, 2001.
11. Evans J. V. Satellite Systems for Personal Communication. *Proc. IEEE*, 1998, vol. 86, no. 7, pp. 1325–1341.
12. Wu W. W. Satellite Communication. *Proc. IEEE*, 1997, vol. 85, no. 6, pp. 998–1010.
13. Fontan F. P., Gonzalez J. P., Ferreiro M. J. S., Castro M. A. V., et al. Complex Envelope Three-state Markov Model Based Simulator for the Narrow-Band LMS Channel. *Int. J. Satellite Communications*, 1997, vol. 15, no. 1, pp. 1–15.

red data. This comparison was shown in Fig. 11 for Westminster and for Guildford, where the corresponding experimental data were plotted by dots.

Conclusion

Even with the data on terrain features using average parameters of the built-up terrain, not the local parameters, we obtained a satisfactory agreement between the theoretical prediction based on both, the Saunders — Evans physical-statistical and multi-parametric stochastic models, and experimental data. This means that the designers of satellite-land links do not need every time to have information on the local built-up terrain parameters as shown in Fig. 6 and 7. It is enough to obtain average parameters of the terrain during satellite movements above the corresponding city, town, village, and so on, and we can for prediction of fading effects to use the stochastic multi-parametric approach.

As can be finally expected, and as seen from Fig. 11, according to the knowledge of the kind of terrain topography from good (open) to bad (urban) scenarios, the main difference is noticeable in the urban environment (as the worst case of strong fading), due to its special propagation features such as multiple diffraction, scattering and reflection from buildings surrounding the subscriber ground-based antenna.

14. Barts R. M., Stutzman W. L. Modeling and Simulation of Mobile Satellite Propagation. *IEEE Trans. Antennas Propagat.*, 1992, vol. 40, no. 4, pp. 375–382.
15. Loo C., Butterworth J. S. Land Mobile Satellite Channel Measurements and Modeling. *Proc. IEEE*, July 1998, vol. 86, no. 7, pp. 1442–1462.
16. Vatalaro F., Mazzenga F. Statistical Channel Modeling and Performance Evaluation in Satellite Personal Communications. *Int. J. Satellite Communications*, 1998, vol. 16, no. 2, pp. 249–255.
17. Loo C. A Statistical Model for Land Mobile Satellite Link. *IEEE Trans. Veh. Technol.*, 1985, vol. VT-34, no. 3, pp. 122–127.
18. Patzold M., Killat U., Laue F. An Extended Suzuki Model for Land Mobile Satellite Channels and its Statistical Properties. *IEEE Trans. Veh. Technol.*, 1998, vol. 47, no. 2, pp. 617–630.
19. Corazza G. E., Vatalaro F. A Statistical Model for Land Mobile Satellite Channels and its Application on Non-Geostationary Orbit Systems. *IEEE Trans. Veh. Technol.*, 1994, vol. 43, no. 3, pp. 738–741.
20. Xia Y., Fang Y. A General Statistical Channel Model for Mobile Satellite Systems. *IEEE Trans. Veh. Technol.*, 2000, vol. 49, no. 3, pp. 744–752.
21. Abdi A., Lau W. C., Alouini M.-S., and Kaveh M. A New Simple Model for Land Mobile Satellite Channels: First- and Second-order Statistics. *IEEE Trans. Wireless Communications.*, 2003, vol. 2, no. 3, pp. 519–528.
22. Saunders S. R., and Evans B. G. A Physical Model of Shadowing Probability for Land Mobile Satellite Propagation. *Electronics Letters*, 1996, vol. 32, no. 17, pp. 1548–1549.
23. Tzaras C., Saunders S. R., and Evans B. G. A Tap-Gain Process for Wideband Mobile Satellite PCN Channels. *Proc. COST 252/259 Joint Workshop*, Bradford, UK, April 21–22, 1998, pp. 156–161.
24. Lutz E., Cygan D., Dippold M., Dolainsky F., Papke W. The Land Mobile Satellite Communication Channel-Recording, Statistics and Channel Model. *IEEE Trans. Veh. Technol.*, 1991, vol. 40, no. 2, pp. 375–385.
25. Butt G., Evans B. G., and Richharia M. Narrowband Channel Statistics from Multiband Propagation Measurements Applicable to High Elevation Angle Land-Mobile Satellite Systems. *IEEE Trans. Select. Areas Commun.*, 1992, vol. 10, no. 8, pp. 1219–1226.
26. Parks M. A. N., Evans B. G., Butt G., and Buonomo S. Simultaneous Wideband Propagation Measurements for Mobile Satellite Communication Systems at L- and S-bands. *Proc. 16th Int. Commun. Systems Conf.*, Washington DC, 1996, pp. 929–936.
27. Karasawa Y., Kimura K., and Minamisono K. Analysis of Availability Improvement in LMSS by Means of Satellite Diversity Based on Three-state Propagation State Model. *IEEE Trans. Veh. Technol.*, 1997, vol. 46, no. 4, pp. 1047–1056.

УДК 621.371

doi:10.15217/issn1684-8853.2018.1.74

Влияние поверхности земли с застройкой на операционные параметры сигналов в каналах связи «Земля — спутник»

Блаунштейн Н. Ш.^а, доктор физ.-мат. наук, профессор, nathan.blaunstein@hotmail.com

Сергеев М. Б.^б, доктор техн. наук, профессор, mbse@mail.ru

Ненашев В. А.^б, канд. техн. наук, доцент, nenashev.va@gmail.com

^аНегевский университет им. Бен-Гуриона, Р.О.В. 653, 1, Бен-Гуриона ул., г. Беэр-Шева, 74105, Израиль

^бСанкт-Петербургский государственный университет аэрокосмического приборостроения, Б. Морская ул., 67, Санкт-Петербург, 190000, РФ

Цель: анализ распространения радиосигналов в городской среде для различной направленности (элевации) движущейся спутниковой антенны и стационарных антенн пользователей, расположенных как ниже, так и выше крыш домов. Задача решалась с помощью стохастического многопараметрического подхода при сосредоточенности на временных и пространственных свойствах изменения мощности сигнала для прогноза потерь в канале и эффектов фединга. **Результаты:** на основе стохастического подхода, предложенного в работе, проанализированы полная мощность сигнала, соответствующие функции плотности вероятности, а также масштабы временных и частотных характеристик. Все прогнозируемые характеристики проанализированы численно, влияние плотности застройки домов и элевации спутниковой антенны на вышеуказанные характеристики проанализированы через призму специальных экспериментов, проведенных многими исследователями. **Практическая значимость:** просчитанные и наблюдаемые экспериментально данные показывают хорошее соответствие между предлагаемым стохастическим подходом и подходами, предложенными другими исследователями, поэтому представленный подход можно использовать для прогноза потерь в канале связи для среды с различным профилем застройки домов и для различных элеваций движущейся спутниковой антенны.

Ключевые слова — канал «Земля — спутник», стохастический многопараметрический подход, профиль застройки и плотности застройки домов, вероятность мультипликативного фединга, потери в канале, расчет канала связи.

Цитирование: Blaunstein N. S., Sergeev M. B., Nenashev V. A. Impact of Built-up Terrain on Operational Parameters of Signals in Land-Satellite Communication Links// Информационно-управляющие системы. 2018. № 1. С. 74–84. doi:10.15217/issn1684-8853.2018.1.74

Citation: Blaunstein N. S., Sergeev M. B., Nenashev V. A. Impact of Built-up Terrain on Operational Parameters of Signals in Land-Satellite Communication Links. *Informatsionno-upravliaiushchie sistemy* [Information and Control Systems], 2018, no. 1, pp. 74–84. doi:10.15217/issn1684-8853.2018.1.74